transferrin (Sigma-Aldrich) in conditioned medium. To remove remaining surface-bound biotin–transferrin, cells were washed three times with Hank's balanced salt solution, pH 4.0. To determine the level of surface-bound transferrin, the treated cells were incubated for 30 min with biotin–transferrin at 4 °C and washed three times with Hank's balanced salt solution, pH 7.4 (*26*). The resulting cell lysates were separated by SDS–PAGE and transferred to the PVDF membrane. Biotin–transferrin was detected by neutravidin–horseradish peroxidase (Pierce). The level of endocytosis in each condition was expressed as of the ratio of internalized vs surface-bound transferrin (*31*).

RESULTS

The Cell-Free Assay Constitutes Bona Fide ϵ- and γ-Cleavages by PS/γ-Secretase. βAPP, a type 1 transmembrane protein, undergoes PS-dependent proteolysis in its transmembrane domain, following "shedding" of the extracellular domain at β- or α-sites (*11*). The intramembrane proteolysis is composed of at least two distinct proteolytic cleavages (dual cleavage), namely, at the ϵ- and γ-sites (Figure 1A) (*2*).

To determine whether the precision of cleavage in intramembrane proteolysis by each PS/γ-secretase is homogeneous in cells, we established a cell-free γ-secretase assay using a detergent-free membrane fraction (Figure 1) (*28*). First, de novo AICD generation from carboxyl-terminal fragment (CTF) stubs of βAPP was analyzed (Figure 1B,C). Following a 20 min metabolic labeling of K293 cells stably expressing βAPP sw and a 30 min chase, we extracted CMFs from the cells and incubated them under various conditions (cell-free incubation). To detect the C-terminus of βAPP, cell lysates were immunoprecipitated with rabbit antiserum 6618, separated by SDS–PAGE, and analyzed by autoradiography. As shown in Figure 1B, during cell-free incubation of the purified CMF, radiolabeled CTF stubs of βAPP rapidly underwent endoproteolysis and concomitantly generated labeled AICD. Termination of the PS function by either exogenous expression of the PS1 dominant negative mutant (D385N) (*32*) or by addition of a specific γ-secretase inhibitor to CMF (Figure 1C) inhibited generation of AICD.

We next examined the precision of both ϵ- and γ-cleavages in the cell-free assay using IP-MS analysis (Figure 1D). We first examined the molecular species of AICD generated during cell-free incubation. The IP-MS analysis showed that the MS profile of AICD was consistent with that previously reported (Figure 1D, left panel) (*7–9*). In addition, the MS spectrum of Aβ generated during cell-free incubation (Figure 1D, right panel) was almost identical to that of Aβ present in the conditioned medium just before extraction of the CMF (data not shown). We therefore conclude that the cleavages in the cell-free assay constitute bona fide PS-dependent ϵ- and γ-cleavages (Figure 1E).

The Precision of ϵ-Cleavage Drastically Changes upon Inhibition of Endocytosis. Proteolysis by PS/γ-secretase occurs on cell organelles including the PM and endosomes before and after endocytosis (*33*). Here, we focused on whether the precision of ϵ- and γ-cleavage changes upon inhibition of endocytosis. To inhibit endocytosis, we used the "tet-off system" (Clontech) in which the expression of the dynamin-1 (Dyn-1) dominant negative mutant K44A is induced by tetracycline withdrawal (tet (−) treatment) in HeLa cells (Figure 2A) (*26*). We first examined the extent to which this mutant suppresses endocytosis of the transferrin receptor. We found that expression of Dyn-1 K44A inhibited the intracellular uptake of biotinylated transferrin (Figure 1 in Supporting Information) by approximately 87 ± 2% (Figure 2B).

Next, we analyzed the ϵ-cleavage in the cell-free γ-secretase assay using CMF from cells cultured with or without tetracycline (Figure 2C,D). Unlike the analysis of K293 cells, the mass spectral analysis showed that AICDϵ51 was a major species formed by CMF from HeLa cells stably expressing

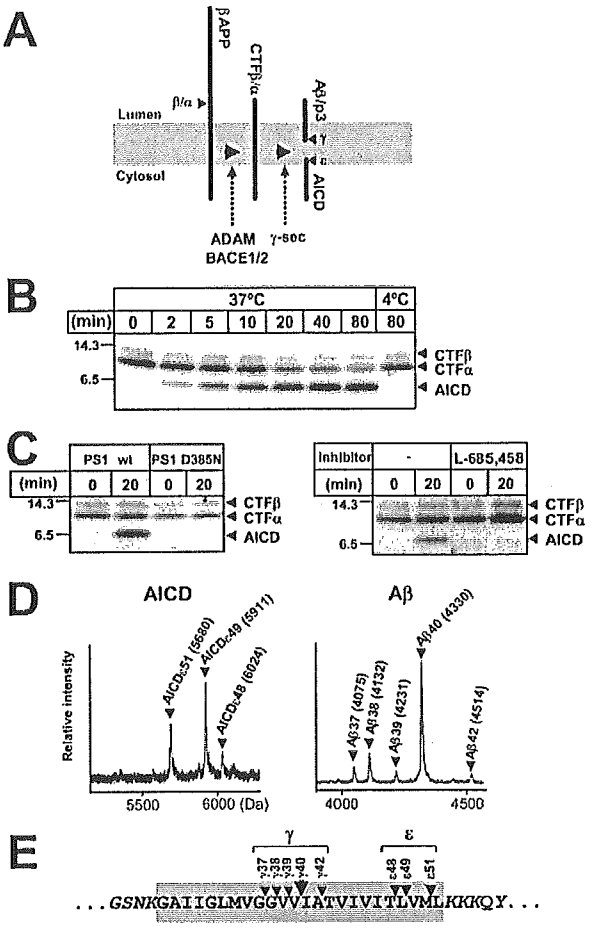

FIGURE 1: Generation of de novo AICD and Aβ in the cell-free γ-secretase assay. (A) Schematic representation of dual cleavage of the βAPP transmembrane domain. See Results for details. (B) Analysis of cell-free γ-secretase assay products by immunoprecipitation/autoradiography using CMF from cells stably expressing βAPP sw. Note that the ~7 kDa product (AICD) was generated over time along with a concurrent reduction in the level of substrates (CTF stubs of βAPP). (C) Analysis of cell-free γ-secretase assay products by immunoprecipitation/autoradiography using CMFs from (i) cells expressing a dominant negative PS1 mutant (PS1 D385N) or (ii) cells treated with or without 10 μM L685,458. (D) Molecular species of de novo AICD and Aβ generated in the cell-free assay. Molecular weights of de novo AICD (left panel) and Aβ (right panel) are shown. Following a 20 min cell-free incubation, the soluble fraction of CMF was immunoprecipitated with antibody 6618 (left panel) or 4G8 (right panel). Panels B–D show representative data from more than three independent experiments. (E) Schematic representation of the ϵ- and γ-cleavages of βAPP. Arrowheads indicate the cleavage sites found in the assay.

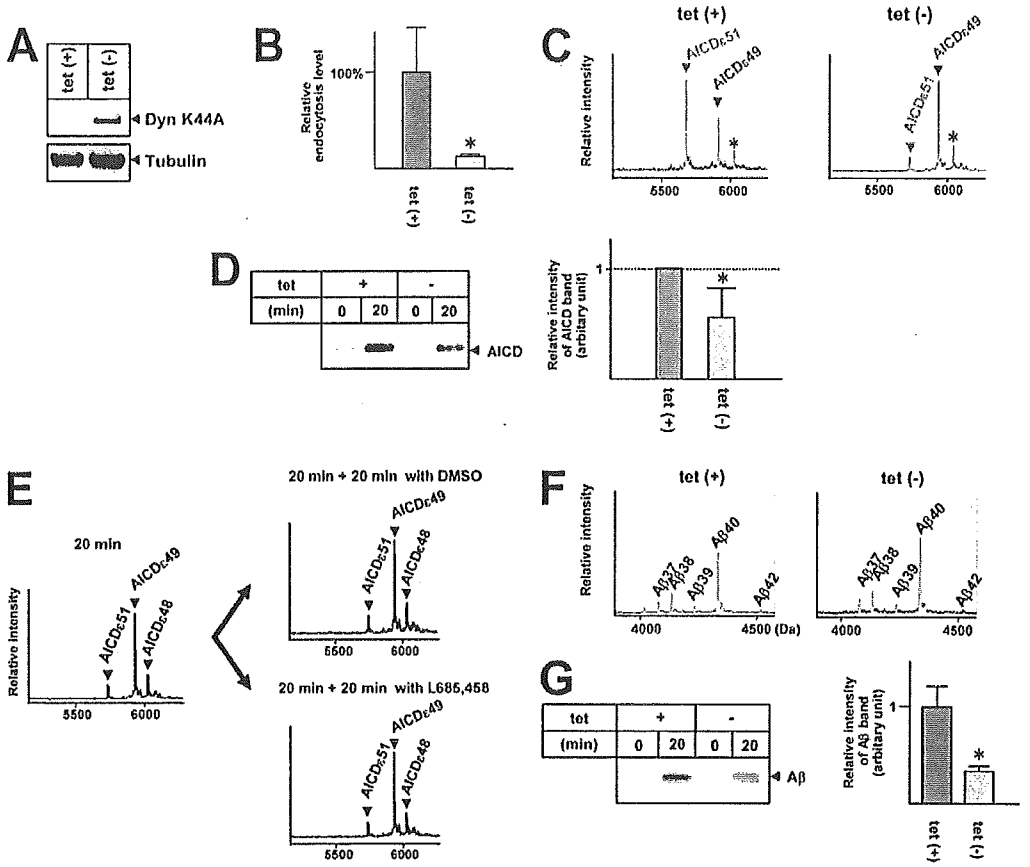

FIGURE 2: Effects of Dyn-1 K44A expression in HeLa cells on the cell-free γ-secretase assay. (A) Induction of Dyn-1 K44A expression. Cells were treated without (−) or with (+) tetracycline, and cell lysates were immunoblotted with 12CA5 (upper panel) or anti-tubulin (lower panel). The results show that Dyn-1 K44A is induced by removal of tetracycline. (B) Inhibition of endocytosis by Dyn-1 K44A expression. The ratio of internalized transferrin at 37 °C to cell surface bound transferrin at 4 °C in cells not expressing Dyn-1 K44A (tet(+)) was defined as 100%. The ratio of endocytosis decreased to 13 ± 2% when the expression of the mutant was induced (tet(−)). The asterisk indicates statistical significance ($P < 0.05$ by Student's t-test). (C) Mass spectra of cell-free generated AICD species. The CMFs from HeLa cells expressing βAPP sw cultured with or without tetracycline were incubated in the cell-free assay. Asterisks indicate the AICDϵ48 species. (D) The level of AICDs generated in the cell-free assay. The AICDs generated in cell-free assays were immunoprecipitated and immunoblotted with the 6618 antiserum (left panel). The intensity of each AICD band was measured by chemiluminescence (right panel). Generation of de novo AICDs was defined as the difference of the AICD band intensities with or without a 20 min cell-free incubation. The asterisk indicates statistical significance ($P < 0.01$ by Student's t-test). (E) Molecular species of AICD observed after a first (left panel) and a second 20 min incubation with L685,458 (lower right panel) or vehicle control DMSO (upper right panel) using CMF from HeLa cells expressing βAPP sw cultured without tetracycline. (F) Mass spectra of the Aβ species generated in the cell-free reaction. The samples were the same as those analyzed in panel C. (G) The level of Aβ produced in the cell-free assay. The Aβ generated in the cell-free assay was analyzed by immunoprecipitation, followed by immunoblotting with the 4G8 antibody (left panel). The intensity of each Aβ band was measured by chemiluminescence (right panel). The asterisk indicates statistical significance ($P < 0.01$ by Student's t-test). In (A), (C), (E), and (F) and in the left panels of (D) and (G), the results are representative data of more than three independent experiments. The results in (B) and the right panels of (D) and (G) indicate the means ± standard deviations of at least triplicate determinations. tet = tetracycline.

βAPP sw in our cell-free assay (Figure 2C, left panel, and Figure 3A, right panel). Surprisingly, expression of Dyn-1 K44A greatly increased the peak height of AICDϵ49 relative to that of AICDϵ51, indicating a change in the precision of ϵ-cleavage upon inhibition of endocytosis (Figure 2C; see also Table 1). A very similar large relative increase of the peak height of AICDϵ49 compared to that of AICDϵ51 was also observed upon addition of 100 nM bafilomycin A1 (Figure 2B in Supporting Information), which inhibited endocytosis by approximately 69 ± 5% (Figures 1 and 2A in Supporting Information) (*34*). Moreover, we found that the relative ratio of the AICDϵ49 peak height to that of AICDϵ51 semiquantitatively correlated with the relative amount of each AICDϵ49 species, indicating that AICDϵ49 and AICDϵ51 have similar ionization efficiencies in the matrix-associated laser desorption ionization/time-of-flight mass spectrometry (see Figure 3 in Supporting Information). We also examined whether the level of ϵ-cleavage changes upon inhibition of endocytosis by immunoblotting (Figure 2D). We detected a significant decrease in intensity of the AICD band upon Dyn-1 K44A expression, indicating that the level of ϵ-cleavage decreases upon inhibition of endocytosis. These findings suggest that inhibition of endocytosis causes a drastic change in the precision of ϵ-cleavage.

We further investigated whether both AICDϵ51 and AICDϵ49 are, indeed, direct products of PS/γ-secretase. We first generated de novo AICD by a 20 min cell-free incubation (Figure 2E, left panel). The solution was further incubated for 20 min with (Figure 2E, lower right panel) or without (Figure 2E, upper right panel) the γ-secretase

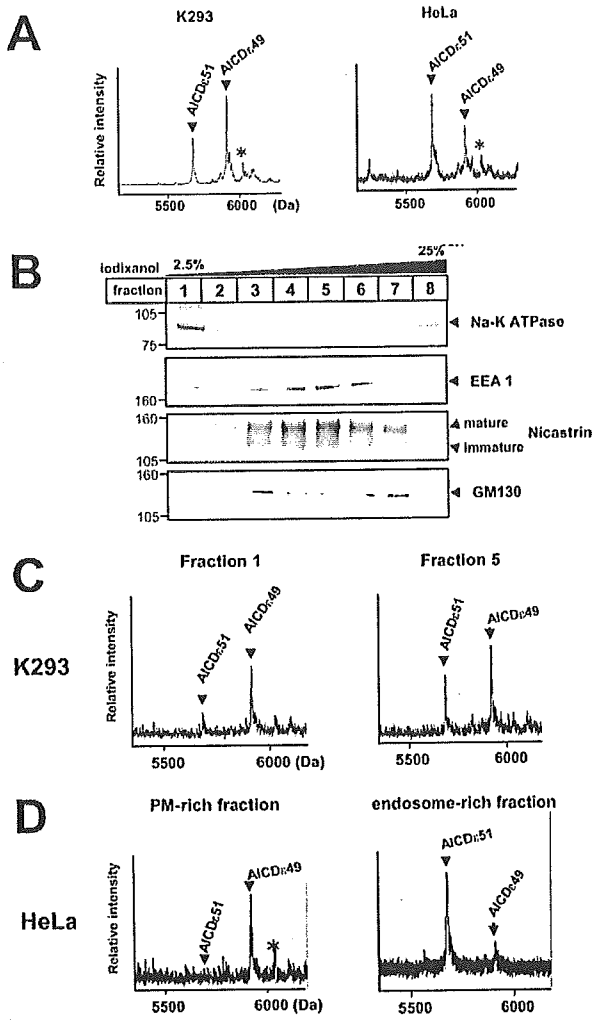

FIGURE 3: Cell-free γ-secretase assay using PM- and endosome-rich fractions. (A) Mass spectra of de novo AICD generated in the cell-free assay using whole CMFs from K293 (left panel) and HeLa (right panel) cells. Asterisks indicate AICDϵ48 species. (B) Postnuclear supernatant fractions of βAPP sw-expressing K293 cells were separated by iodixanol gradient centrifugation and analyzed by immunoblotting using antibodies to organelle marker proteins. (C) Mass spectra of de novo AICD generated by fractions 1 and 5 from K293 cells. (D) Mass spectra of de novo AICD generated by PM- or endosome-rich fractions from HeLa cells expressing βAPP sw. Results in (A) to (D) are representative of more than three independent experiments.

inhibitor L685,458. This inhibitor neither increased the relative peak height of AICDϵ51 nor reduced that of AICDϵ49/AICDϵ48, suggesting that AICDϵ51 is not a degradation product of AICDϵ49/AICDϵ48 but rather is generated directly by PS/γ-secretase.

These results indicated that there is a striking change in the precision of ϵ-cleavage upon inhibition of endocytosis. We therefore examined whether there is also a parallel remarkable change in the precision of γ-cleavage. We chose IP-MS analysis in order to observe all of the de novo Aβ species. In clear contrast to the analysis of AICD (Figure 2C), IP-MS analysis did not reveal drastic differences in the profiles of de novo Aβ species (i.e., Aβ37, Aβ38, Aβ39, Aβ40, and Aβ42) between reactions using CMF from control cells (Figure 2F, left panel) and cells expressing Dyn-1 K44A (Figure 2F, right panel). Also, very similar results were observed upon inhibition of endocytosis by bafilomycin A1 (Figure 2C in Supporting Information). Immunoprecipitation/immunoblotting analysis for detecting Aβ species revealed a significant decrease upon expression of Dyn-1 K44A (Figure 2G). Thus, in parallel to AICD, we detected a decrease in the level of de novo Aβ levels in the presence of Dyn-1 K44A expression. These results indicated a concomitant decrease in both ϵ- and γ-cleavage efficiencies by PS/γ-secretase upon inhibition of endocytosis.

The Precision of ϵ-Cleavage in the PM-Rich Fractions Is Distinct from That in the Endosome-Rich Fractions. Our cell-free γ-secretase assay revealed that inhibition of endocytosis by expression of the Dyn-1 K44A mutant causes a drastic change in the precision of ϵ-cleavage by PS/γ-secretase but does not concurrently cause such a change in the precision of γ-cleavage. This prompted us to investigate whether there are differences in the precision of ϵ-cleavage on the PM and endosomes. Using CMFs from K293 and HeLa cells, we performed cell-free γ-secretase assays and examined the mass spectra of the generated AICD. As described above (Figures 1D and 2C), in unstimulated K293 and HeLa cells, the relative amounts of ϵ49 and ϵ51 produced are different, indicating that the precision of cleavage at the ϵ-site is distinct in the two cell lines (Figure 3A).

We next examined the production of AICD species in PM- and endosome-rich fractions isolated by iodixanol density gradient centrifugation from CMF prepared from K293 cells expressing βAPP sw. Na−K ATPase, a marker of PM, was detected primarily in the lightest fraction (fraction 1; Figure 3B, first panel), whereas the early endosome markers early endosome antigen 1 (Figure 3B, second panel) and matured nicastrin (Figure 3B, third panel) were detected together in higher density fractions (fractions 4 and 5). GM130, a marker of Golgi, was found mainly in fractions 3 and 7 (Figure 3B, fourth panel). These results suggest that fractions 1 and 5 are the PM- and endosome-rich fractions, respectively. When these fractions were employed in the cell-free γ-secretase assay, we found that the peak height of AICDϵ51 relative to that of AICDϵ49 was larger in the endosome-rich fraction than in the PM-rich fraction (Figure 3C). In contrast, the peak height of AICDϵ49 relative to that of AICDϵ51 was higher in the PM-rich fraction than the endosome-rich fraction (Figure 3C). Similarly, using membrane fractions from HeLa cells, we found that AICDϵ49 was the dominant product in PM-rich fractions, whereas AICDϵ51 was the main product in endosome-rich fractions. These results indicate that the precision of ϵ-cleavage differs on PM and endosomes. Specifically, cleavage at ϵ49, which lies deeper inside the transmembrane domain, tends to occur more on PM than endosomes, whereas the opposite is true for cleavage at ϵ51, which lies closer to the cytosolic side and the interface between transmembrane and intracellular domains.

The Precision of ϵ-Cleavage Is Affected by pH. Our results show that the precision of cleavage at the ϵ-site changes drastically upon inhibition of endocytosis and is affected by the subcellular location. The process of cleavage by PS/γ-secretase may therefore change according to the surrounding conditions. For this reason, we examined whether changing the pH during the cell-free γ-secretase assay affects the level and precision of ϵ- and γ-cleavage. IP-MS showed that, when

Table 1: Amino Acid Sequences of AICDϵ49 and AICDϵ51 Species

MW (obsd)	species	sequence	MW (calcd)
5911	AICDϵ49	V^{646}MLKKKQYTSIHHGVVEVDAAVTPEERHLSKMQQNGYENPTYKFFEQMQN^{695}	5910.7
5680	AICDϵ51	L^{648} KKKQYTSIHHGVVEVDAAVTPEERHLSKMQQNGYENPTYKFFEQMQN^{695}	5680.4

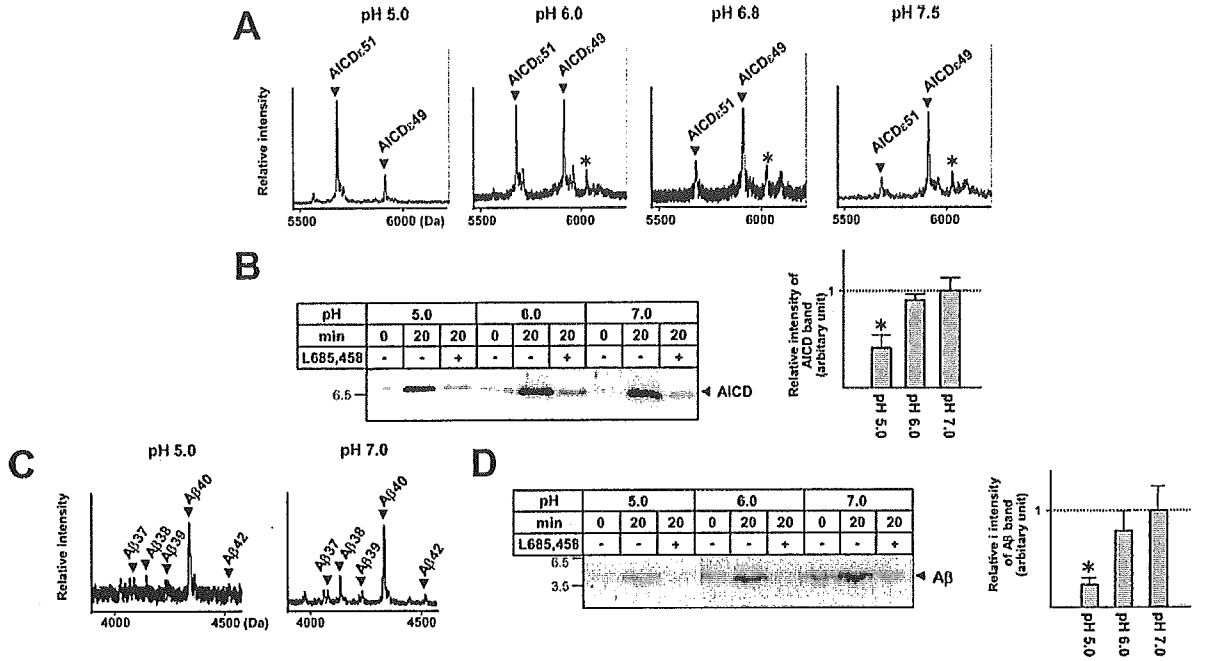

FIGURE 4: Effects of pH on ϵ- and γ-cleavage. (A) Mass spectra of AICD generated in the cell-free assay at pHs between 7.5 and 5.0. CMFs from βAPP sw-expressing K293 cells were resuspended in reaction buffer at the indicated pH. Asterisks indicate AICDϵ48 species. (B) The level of AICDs generated at various pHs. The cell-free incubation was performed in the presence of either L685,458 or vehicle alone (DMSO) (left panel). The asterisk indicates that the intensity of the AICD band at pH 5.0 was statistically lower than those at pH 6.0 and 7.0 ($P < 0.01$ by Student's *t*-test). (C) Mass spectra of Aβ generated in the cell-free assay at pH 5.0 and 7.0. (D) The level of Aβ generated at various pHs and in the presence of L685,458 or vehicle control (DMSO). The asterisk indicates statistical significance ($P < 0.01$ by Student's *t*-test). In (A) and (C) and the left panels of (B) and (D), the results are representative of more than three independent experiments. In the right panels of (B) and (D), the results indicate the means ± standard deviations from at least triplicate determinations.

we changed the buffer pH from 7.5 to 5.0, the relative cleavage efficiency at the ϵ49 and ϵ51 sites changed (Figure 4A). The more acidic the pH, the higher the AICDϵ51 peak became, demonstrating that the pH affects cleavage at the ϵ-site. Immunoblotting also showed that lowering the pH to 5.0 decreased the amount of AICD produced, indicating a reduction in the total amount of cleavage at the ϵ-site (Figure 4B). De novo AICD production was almost completely suppressed by an inhibitor of PS-dependent γ-secretase (L685,458) at various pHs. Therefore, the AICD production that we observed was mostly due to proteolysis by PS-dependent γ-secretase (Figure 4B). These results indicate that alteration of the pH affects both the precision and the level of ϵ-site cleavage. We also studied the effect of pH on the precision and amount of γ-site cleavage. As shown in Figure 4C, we could not detect any ϵ-cleavage-like changes in the precision of γ-cleavage. Also, lowering the pH to 5.0 caused a reduction in the total amount of de novo Aβ production (Figure 4D). Therefore, lowering the pH reduced the level of cleavage at both the γ- and ϵ-sites. Collectively, these results show that the pH in the cell-free assay affects the precision of cleavage at the ϵ-site.

DISCUSSION

In this study, we investigated intramembrane proteolysis of βAPP and demonstrated dynamic changes in the precision of cleavage by the PS/γ-secretase. Using a cell-free γ-secretase assay, we showed that the precision of ϵ-site cleavage changes depending on the subcellular location and pH. These results suggest that the precision of cleavage by the PS/γ-secretase complex can be regulated physiologically.

Inhibition of endocytosis also induced a change in the precision of ϵ-cleavage, suggesting that the function of PS/γ-secretase is related to endocytosis. The precision of ϵ-cleavage on PM and endosomes differs, demonstrating that the function of PS/γ-secretase may be heterogeneous in cells. It is unlikely that the change in precision of ϵ-cleavage observed in this study is due to differences in the thickness of PM and endosome membranes because very similar changes were caused by altering the pH in the cell-free assay. Moreover, our results suggest that the precision of ϵ-cleavage is more dynamic than that of γ-cleavage. Therefore, our results can be explained by (i) additional physiological factors that interact with the active PS/γ-secretase complex or (ii) altered substrate recognition/access at different pH conditions that exist at the plasma membrane and endosomes.

Because the PS/γ-secretase complex mediates both γ- and ϵ-cleavages in the transmembrane domain of βAPP (*2*), one might predict that the processes of γ- and ϵ-cleavage would behave the same. Previous results have shown, however, that the effects of PS mutations on the relative levels of γ42 and

ϵ-site cleavages do not always correlate (*17*). Furthermore, in the current study, we showed that the precision of ϵ- and γ-site cleavages on PM and endosomes did not change in parallel. Our results support the hypothesis that the ϵ-cleavage process is distinct from that of the γ-cleavage, although both occur on the same transmembrane domain and are mediated by the same PS-dependent γ-secretases.

Recent reports have described the existence of several long Aβ species that are thought to be membrane-bound remnants from ϵ-cleavage of CTF stubs (*35*−*37*). Also, it has been reported that there is an association between the cleavages at ϵ51 and at γ42, which are types of ϵ- and γ-site cleavages, respectively (*16*). These findings indicate that there is a time-dependent relationship between γ- and ϵ-cleavages, namely, that γ-cleavage follows ϵ-cleavage (*36*, *37*). If this is generally true, de novo AICD and Aβ is generated from distinct substrates in our cell-free assay; in other words, AICDs is generated from CTF stubs of βAPP, whereas Aβ must be generated from long and membrane-bound Aβ. Otherwise, our results suggest that the process determining the precision of ϵ-cleavage is distinct from that for the γ-cleavage. Thus, it appears that the time-dependent association between γ- and ϵ-cleavages either is not dominant but rather simply reflects the rate of each cleavage under physiological conditions.

In our cell-free assay, conditions mimicking physiological cell functions (i.e., changes in subcellular location, endocytosis, and pH) affected the efficiency of cleavage at ϵ49 and ϵ51; however, we could not find any consistent correlations between relative peak heights of AICDϵ48 and those of AICDϵ49 or AICDϵ51, even though AICDϵ48 was one of the major species.

In summary, we demonstrate here that the precision of ϵ-cleavage of βAPP changes depending on endocytotic function. In future studies, we will examine whether similar changes in the precision of PS-mediated cleavage in the TM-C also occur for other substrates, such as Notch-1.

ACKNOWLEDGMENT

We thank Drs. Harald Steiner, Masaki Nishimura, Maho Morishima-Kawashima, and Yasuo Ihara for critically reading the manuscript. We also thank Drs. Sandra L. Schmid and Takeshi Baba for providing Dyn-1 K44A-expressing HeLa cells.

SUPPORTING INFORMATION AVAILABLE

Four figures indicating that (i) inhibition of endocytosis by bafilomycin A1 treatment caused a drastic change of ϵ-cleavage precision, (ii) the relative ratio of the AICDϵ49 peak height to that of AICDϵ51 semiquantitatively correlated with the relative amount of each AICD species, and (iii) wt βAPP as well as βAPP sw caused the drastic change in the precision of ϵ-cleavage. This material is available free of charge via the Internet at http://pubs.acs.org.

REFERENCES

1. Selkoe, D., and Kopan, R. (2003) Notch and presenilin: regulated intramembrane proteolysis links development and degeneration, *Annu. Rev. Neurosci. 26*, 565−597.
2. Haass, C. (2004) Take five-BACE and the gamma-secretase quartet conduct Alzheimer's amyloid beta-peptide generation, *EMBO J. 23*, 483−488.
3. Okochi, M., Steiner, H., Fukumori, A., Tanii, H., Tomita, T., Tanaka, T., Iwatsubo, T., Kudo, T., Takeda, M., and Haass, C. (2002) Presenilins mediate a dual intramembranous gamma-secretase cleavage of Notch-1, *EMBO J. 21*, 5408−5416.
4. Lammich, S., Okochi, M., Takeda, M., Kaether, C., Capell, A., Zimmer, A. K., Edbauer, D., Walter, J., Steiner, H., and Haass, C. (2002) Presenilin-dependent intramembrane proteolysis of CD44 leads to the liberation of its intracellular domain and the secretion of an Abeta-like peptide, *J. Biol. Chem. 277*, 44754−44759.
5. Okochi, M., Fukumori, A., Jiang, J., Itoh, N., Kimura, R., Steiner, H., Haass, C., Tagami, S., and Takeda, M. (2006) Secretion of the Notch-1 Abeta-like peptide during Notch signaling, *J. Biol. Chem.* (in press).
6. Sastre, M., Steiner, H., Fuchs, K., Capell, A., Multhaup, G., Condron, M. M., Teplow, D. B., and Haass, C. (2001) Presenilin-dependent gamma-secretase processing of beta-amyloid precursor protein at a site corresponding to the S3 cleavage of Notch, *EMBO Rep. 2*, 835−841.
7. Chen, F., Gu, Y., Hasegawa, H., Ruan, X., Arawaka, S., Fraser, P., Westaway, D., Mount, H., and St George-Hyslop, P. (2002) Presenilin 1 mutations activate gamma 42-secretase but reciprocally inhibit epsilon-secretase cleavage of amyloid precursor protein (APP) and S3-cleavage of notch, *J. Biol. Chem. 277*, 36521−36526.
8. Yu, C., Kim, S. H., Ikeuchi, T., Xu, H., Gasparini, L., Wang, R., and Sisodia, S. S. (2001) Characterization of a presenilin-mediated amyloid precursor protein carboxyl-terminal fragment gamma. Evidence for distinct mechanisms involved in gamma-secretase processing of the APP and Notch1 transmembrane domains, *J. Biol. Chem. 276*, 43756−43760.
9. Gu, Y., Misonou, H., Sato, T., Dohmae, N., Takio, K., and Ihara, Y. (2001) Distinct intramembrane cleavage of the beta-amyloid precursor protein family resembling gamma-secretase-like cleavage of Notch, *J. Biol. Chem. 276*, 35235−35238.
10. Weidemann, A., Eggert, S., Reinhard, F. B., Vogel, M., Paliga, K., Baier, G., Masters, C. L., Beyreuther, K., and Evin, G. (2002) A novel epsilon-cleavage within the transmembrane domain of the Alzheimer amyloid precursor protein demonstrates homology with Notch processing, *Biochemistry 41*, 2825−2835.
11. Selkoe, D. J. (2001) Alzheimer's disease: genes, proteins, and therapy, *Physiol. Rev. 81*, 741−766.
12. Weggen, S., Eriksen, J. L., Das, P., Sagi, S. A., Wang, R., Pietrzik, C. U., Findlay, K. A., Smith, T. E., Murphy, M. P., Bulter, T., Kang, D. E., Marquez-Sterling, N., Golde, T. E., and Koo, E. H. (2001) A subset of NSAIDs lower amyloidogenic Abeta42 independently of cyclooxygenase activity, *Nature 414*, 212−216.
13. Kukar, T., Murphy, M. P., Eriksen, J. L., Sagi, S. A., Weggen, S., Smith, T. E., Ladd, T., Khan, M. A., Kache, R., Beard, J., Dodson, M., Merit, S., Ozols, V. V., Anastasiadis, P. Z., Das, P., Fauq, A., Koo, E. H., and Golde, T. E. (2005) Diverse compounds mimic Alzheimer disease-causing mutations by augmenting Abeta42 production, *Nat. Med. 11*, 545−550.
14. Lazarov, O., Robinson, J., Tang, Y. P., Hairston, I. S., Korade-Mirnics, Z., Lee, V. M., Hersh, L. B., Sapolsky, R. M., Mirnics, K., and Sisodia, S. S. (2005) Environmental enrichment reduces Abeta levels and amyloid deposition in transgenic mice, *Cell 120*, 701−713.
15. Sato, T., Dohmae, N., Qi, Y., Kakuda, N., Misonou, H., Mitsumori, R., Maruyama, H., Koo, E. H., Haass, C., Takio, K., Morishima-Kawashima, M., Ishiura, S., and Ihara, Y. (2003) Potential link between amyloid beta-protein 42 and C-terminal fragment gamma 49−99 of beta-amyloid precursor protein, *J. Biol. Chem. 278*, 24294−24301.
16. Funamoto, S., Morishima-Kawashima, M., Tanimura, Y., Hirotani, N., Saido, T. C., and Ihara, Y. (2004) Truncated carboxyl-terminal fragments of beta-amyloid precursor protein are processed to amyloid beta-proteins 40 and 42, *Biochemistry 43*, 13532−13540.
17. Moehlmann, T., Winkler, E., Xia, X., Edbauer, D., Murrell, J., Capell, A., Kaether, C., Zheng, H., Ghetti, B., Haass, C., and Steiner, H. (2002) Presenilin-1 mutations of leucine 166 equally affect the generation of the Notch and APP intracellular domains independent of their effect on Abeta 42 production, *Proc. Natl. Acad. Sci. U.S.A. 99*, 8025−8030.
18. Iwatsubo, T. (2004) The gamma-secretase complex: machinery for intramembrane proteolysis, *Curr. Opin. Neurobiol. 14*, 379−383.
19. Yu, G., Nishimura, M., Arawaka, S., Levitan, D., Zhang, L., Tandon, A., Song, Y. Q., Rogaeva, E., Chen, F., Kawarai, T.,

Supala, A., Levesque, L., Yu, H., Yang, D. S., Holmes, E., Milman, P., Liang, Y., Zhang, D. M., Xu, D. H., Sato, C., Rogaev, E., Smith, M., Janus, C., Zhang, Y., Aebersold, R., Farrer, L. S., Sorbi, S., Bruni, A., Fraser, P., and St. George-Hyslop, P. (2000) Nicastrin modulates presenilin-mediated notch/glp-1 signal transduction and betaAPP processing, *Nature 407*, 48−54.

20. Francis, R., McGrath, G., Zhang, J., Ruddy, D. A., Sym, M., Apfeld, J., Nicoll, M., Maxwell, M., Hai, B., Ellis, M. C., Parks, A. L., Xu, W., Li, J., Gurney, M., Myers, R. L., Himes, C. S., Hiebsch, R., Ruble, C., Nye, J. S., and Curtis, D. (2002) aph-1 and pen-2 are required for Notch pathway signaling, gamma-secretase cleavage of betaAPP, and presenilin protein accumulation, *Dev. Cell 3*, 85−97.
21. Wilson, C. A., Doms, R. W., Zheng, H., and Lee, V. M. (2002) Presenilins are not required for A beta 42 production in the early secretory pathway, *Nat. Neurosci. 5*, 849−855.
22. Lai, M. T., Crouthamel, M. C., DiMuzio, J., Pietrak, B. L., Donoviel, D. B., Bernstein, A., Gardell, S. J., Li, Y. M., and Hazuda, D. (2006) A presenilin-independent aspartyl protease prefers the gamma-42 site cleavage, *J. Neurochem. 96*, 118−125.
23. Okochi, M., Ishii, K., Usami, M., Sahara, N., Kametani, F., Tanaka, K., Fraser, P. E., Ikeda, M., Saunders, A. M., Hendriks, L., Shoji, S. I., Nee, L. E., Martin, J. J., Van Broeckhoven, C., St. George-Hyslop, P. H., Roses, A. D., and Mori, H. (1997) Proteolytic processing of presenilin-1 (PS-1) is not associated with Alzheimer's disease with or without PS-1 mutations, *FEBS Lett. 418*, 162−166.
24. Okochi, M., Eimer, S., Bottcher, A., Baumeister, R., Romig, H., Walter, J., Capell, A., Steiner, H., and Haass, C. (2000) A loss of function mutant of the presenilin homologue SEL-12 undergoes aberrant endoproteolysis in *Caenorhabditis elegans* and increases abeta 42 generation in human cells, *J. Biol. Chem. 275*, 40925−40932.
25. Steiner, H., Romig, H., Pesold, B., Philipp, U., Baader, M., Citron, M., Loetscher, H., Jacobsen, H., and Haass, C. (1999) Amyloidogenic function of the Alzheimer's disease-associated presenilin 1 in the absence of endoproteolysis, *Biochemistry 38*, 14600−14605.
26. Damke, H., Baba, T., Warnock, D. E., and Schmid, S. L. (1994) Induction of mutant dynamin specifically blocks endocytic coated vesicle formation, *J. Cell Biol. 127*, 915−934.
27. Mizutani, T., Taniguchi, Y., Aoki, T., Hashimoto, N., and Honjo, T. (2001) Conservation of the biochemical mechanisms of signal transduction among mammalian Notch family members, *Proc. Natl. Acad. Sci. U.S.A. 98*, 9026−9031.
28. Pinnix, I., Musunuru, U., Tun, H., Sridharan, A., Golde, T., Eckman, C., Ziani-Cherif, C., Onstead, L., and Sambamurti, K. (2001) A novel gamma-secretase assay based on detection of the putative C-terminal fragment-gamma of amyloid beta protein precursor, *J. Biol. Chem. 276*, 481−487.
29. McLendon, C., Xin, T., Ziani-Cherif, C., Murphy, M. P., Findlay, K. A., Lewis, P. A., Pinnix, I., Sambamurti, K., Wang, R., Fauq, A., and Golde, T. E. (2000) Cell-free assays for gamma-secretase activity, *FASEB J. 14*, 2383−2386.
30. Okochi, M., Walter, J., Koyama, A., Nakajo, S., Baba, M., Iwatsubo, T., Meijer, L., Kahle, P. J., and Haass, C. (2000) Constitutive phosphorylation of the Parkinson's disease associated alpha-synuclein, *J. Biol. Chem. 275*, 390−397.
31. Chyung, J. H., and Selkoe, D. J. (2003) Inhibition of receptor-mediated endocytosis demonstrates generation of amyloid beta-protein at the cell surface, *J. Biol. Chem. 278*, 51035−51043.
32. Wolfe, M. S., Xia, W., Ostaszewski, B. L., Diehl, T. S., Kimberly, W. T., and Selkoe, D. J. (1999) Two transmembrane aspartates in presenilin-1 required for presenilin endoproteolysis and gamma-secretase activity, *Nature 398*, 513−517.
33. Kimberly, W. T., and Wolfe, M. S. (2003) Identity and function of gamma-secretase, *J. Neurosci. Res. 74*, 353−360.
34. Stevens, T. H., and Forgac, M. (1997) Structure, function and regulation of the vacuolar (H+)-ATPase, *Annu. Rev. Cell Dev. Biol. 13*, 779−808.
35. Zhao, G., Mao, G., Tan, J., Dong, Y., Cui, M. Z., Kim, S. H., and Xu, X. (2004) Identification of a new presenilin-dependent zeta-cleavage site within the transmembrane domain of amyloid precursor protein, *J. Biol. Chem. 279*, 50647−50650.
36. Qi-Takahara, Y., Morishima-Kawashima, M., Tanimura, Y., Dolios, G., Hirotani, N., Horikoshi, Y., Kametani, F., Maeda, M., Saido, T. C., Wang, R., and Ihara, Y. (2005) Longer forms of amyloid beta protein: implications for the mechanism of intramembrane cleavage by gamma-secretase, *J. Neurosci. 25*, 436−445.
37. Zhao, G., Cui, M. Z., Mao, G., Dong, Y., Tan, J., Sun, L., and Xu, X. (2005) gamma-Cleavage is dependent on zeta-cleavage during the proteolytic processing of amyloid precursor protein within its transmembrane domain, *J. Biol. Chem. 280*, 37689−37697.

BI052412W

PSYCHOGERIATRICS 2004; 4: S57–S61

Possible assessment of Alzheimer's γ-secretase activity by level of Aβ-like peptides

Masayasu OKOCHI and Masatoshi TAKEDA

Department of Post-Genomics and Diseases, Division of Psychiatry and Behavioral Proteomics, Osaka University Graduate School of Medicine, 565–0871 Osaka, Japan

Correspondence: Masayasu Okochi, Department of Post-Genomics and Diseases, Division of Psychiatry and Behavioral Proteomics, Osaka University Graduate School of Medicine, 565–0871 Osaka, Japan
Email: mokochi@psy.med.osaka-u.ac.jp

Key words: *Alzheimer's disease, Amyloid β-like peptide, Notch-β peptide, Notch signaling, diagnostic marker.*

The amyloid hypothesis has been one of the popular ideas aimed at explaining pathogenesis of Alzheimer's disease (AD).[1] This posits that the process, by which secreted soluble amyloid β-protein (Aβ) turns into its aggregated insoluble form, is essential for the development of AD. Aβ, which was originally identified biochemically and is always present as insoluble amyloid fibril in senile plaques (SP) of AD brains, was found to be released physiologically from cells in the form of soluble peptides.[2,3] The amyloid hypothesis was a logical solution to this contradiction. Except for unusual conditions, all pathological AD mutants of presenilins (PS) and β-amyloid precursor protein (βAPP) affect the precision of the γ-cleavage site of βAPP,[1] that is, the mutants cause a partial shift of the γ-cleavage site in the direction of the C-terminal with 2~3 amino acids.[1] As a result, the generative ratio of Aβ species ending 42 (Aβ numbering) in relation to that of the major Aβ species ending 40 is up-regulated.[4] SP is also an invariant phenotype of sporadic AD (SAD), and Aβ42 deposition in SP is observed in the majority of AD cases. However, because of the highly aggregative nature of Aβ42, it has been very difficult to determine whether the precision of the γ-cleavage is affected, and thus whether Aβ42 generation is up-regulated in sporadic AD brains. Nevertheless, Aβ42 peptide could be not only, as seen earlier, a substance which regulates the AD pathological process, but theoretically also one of the most effective bio-markers for AD. However, again because of its extremely aggregative nature, the Aβ42 level in CSF or peripheral blood of AD patients usually decreases and does not reflect its generation,[5] which makes it difficult to use this level as a prediagnostic marker of AD.

We recently found that a group of peptides may be secreted by the same mechanism as that for γ-secretase of βAPP.[6,7] We also found that the precision of this cleavage is affected by familial Alzheimer's disease-associated PS1 mutations similar to the pathological endoproteolysis of βAPP.[6] Therefore, by measuring these Aβ-like peptides instead of Aβ, it may be possible to determine whether γ-cleavage of βAPP is affected in the SAD brain. Furthermore, it is theoretically possible that this might lead to the use of peptides levels as a prediagnostic marker for AD.

RIP SIGNALING

Recently, a novel signaling paradigm has been proposed, in which membrane-anchored cell-surface receptors themselves undergo sequential endoproteolysis upon ligand binding and their intracellular domains directly translocate to the nucleus and function as transcription modifiers.[8,9] The biochemical characteristic of such a signaling mechanism is the importance of intramembranous endoproteolysis, which releases the cytosolic domain of the receptor

from membranes.[8,9] That is, fragments which translocate to the nucleus and modify transcription are immediately generated by a special form of intramembranous endoproteolysis. This cleavage is known as regulated intramembranous proteolysis (RIP).[9] RIP is an as yet largely unknown endoproteolysis that can hydrolyze a peptide bond in a highly hydrophobic environment. RIP was first described in connection with the sequential endoproteolysis of sterol regulatory element-binding protein (SREBP) (Fig. 1a),[9] a membrane-bound transcription factor that regulates cholesterol homeostasis.

A type-II membrane-anchored transcriptional factor ATF6, which is activated in ER stress response, has also been shown to be a substrate for the sequential cleavages by S1P and S2P (Fig. 1a).[10] Striking similarities in endoproteolysis of ATF6 and SREBP can easily be found. In both cases, "ectodomain shedding" by S1P triggers intramembranous endoproteolysis by S2P, which in turn generates NTF that translocate to the nucleus.[11] Induction of GRP78, an ER chaperone, is eliminated in cells lacking S2P.[10]

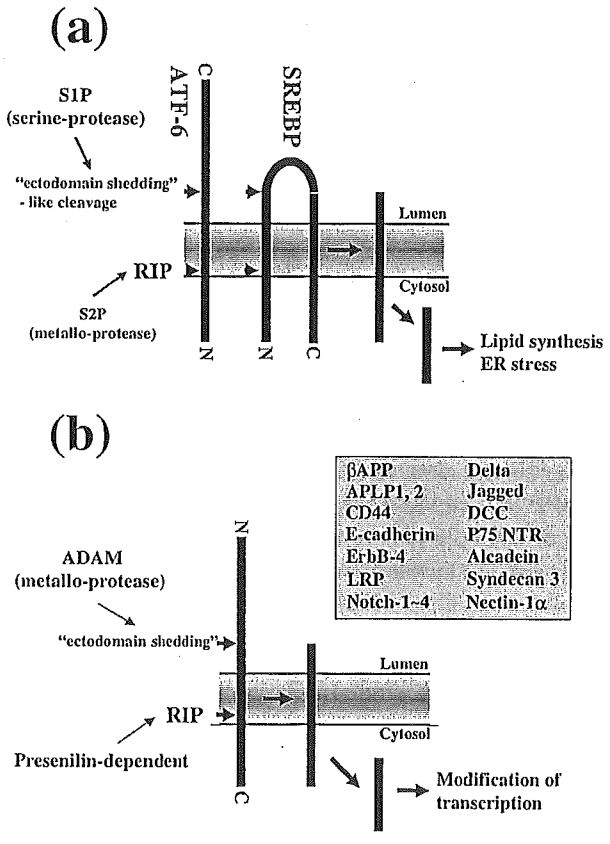

Figure 1 (a) Sequential cleavages of ATF-6 and SREBPs share common features. (b) Common sequential cleavage mechanism (RIP) when substrates share the type-1 topology in their transmembrane domain.

On the other hand, when a disintegrin and metalloprotease (ADAM) and presenilin (PS) dependent γ-secretase mechanism is involved in RIP, the transmembrane domains of the substrate receptors appear to have a type-I topology (see Fig. 1b). In addition to Notch receptors,[12,13] βAPP,[14] ErbB-4,[15] E-Cadherin,[16] LRP,[17] CD44,[7,18] Nectin-1α,[19] Notch ligands, Delta and Jagged,[20,21] DCC,[22] P75 neurotrophin receptor,[23] Alcadein,[24] and Syndecan 3[25] have so far been identified as substrates for this mechanism. Although still controversial, these proteins are basically thought to undergo "extracellular shedding", which is a prerequisite for consecutive PS dependent proteolysis.

PS comprise eight potent transmembrane proteins with both an N- and a C-terminus in cytosol,[26] and occur in high molecular weight complexes consisting of Nicastrin, Pen-2, and Aph-1.[27,28] PS produce γ-secretase activity, which generates both the C-terminus of Aβ and the N-terminus of the βAPP intracellular cytoplasmic domain (AICD).[29] Genomic knock-out of PS1 or PS1/2 causes Notch phenotype *in vivo*, which shows that the major function of PS is to mediate Notch signaling.[30] Notch signaling was found to be a common signaling mechanism for metazoans, which plays an essential role in neural differentiation from ectoderm.[8] Recently, however, this signaling has been found to play various roles during not only development but also adulthood. Notch signaling is realized only when Notch ligands (DSL family proteins) expressed in signaling cells bind to Notch receptors expressed in the signal receiving cells. Upon binding to ligands, Notch receptors undergo sequential endoproteolysis, which results in the release of the cytosolic C-terminal fragment, NICD, which is believed to directly translocate to the nucleus and regulate transcription of target genes.[8]

PHYSIOLOGICAL SECRETION OF Aβ-LIKE FRAGMENTS

We have analyzed in detail the PS-dependent intramembranous proteolysis of Notch-1[6] and CD44[7] and found that, as a result of the endoproteolysis, the Aβ-like Notch (Notch-1 Aβ-like peptide: Nβ) or CD44 (CD44 Aβ-like peptide: CD44β) fragment was extracellularly secreted in the form of NFT[7] (see Fig. 2). This

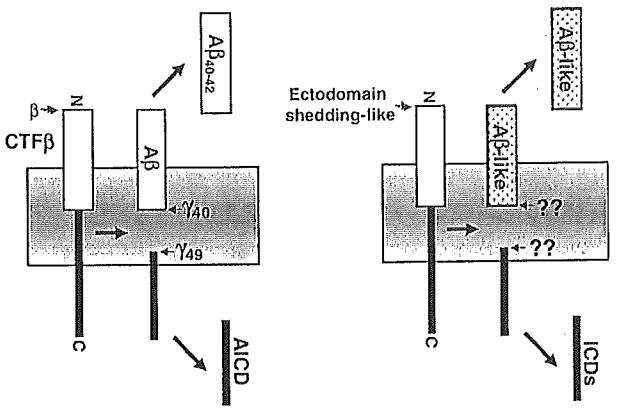

Figure 2 Aβ-like peptides are secreted through signal transduction mediated by presenilin-dependent RIP.

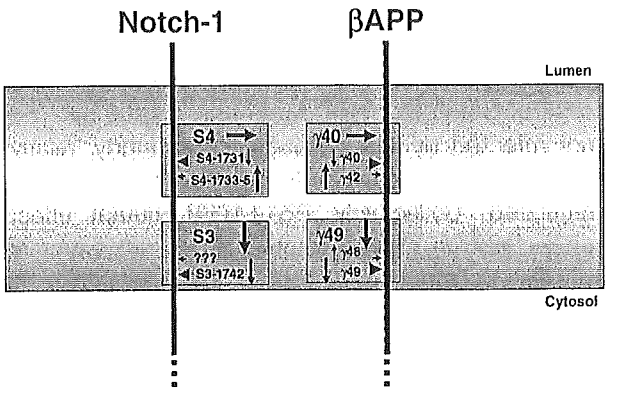

Figure 4 Similar effects of FAD-associated PS mutations on "dual" γ-cleavage of βAPP and Notch-1.

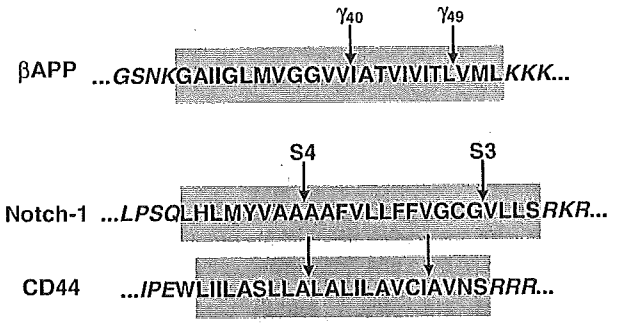

Figure 3 PS-dependent intramembranous proteolysis, which we termed the "Dual Cleavage" mechanism. Arrows indicate proteolytic cleavage sites. Small transmembrane peptides between 2 cleavage sites have not yet been identified.

indicates that at least several peptides that contain a transmembrane domain-like Aβ are secreted *in vivo* (Fig. 2). Therefore, one might suggest that secretion of peptides containing the transmembrane domain may be a phenomenon common to several substrates for PS dependent endoproteolysis. Interestingly, the C-termini of these secreted peptides do not directly correspond to the N-termini of cytosolic CTFs functioning as signaling molecules, but are formed by distinct proteolysis upstream of the N-termini of CTFs (Fig. 2). Thus, intramembranous endoproteolysis, which liberates an Aβ-like peptide, essentially consists of a distinct dual endoproteolysis, which we have termed "Dual Cleavage Mechanism" (Fig. 3).[6,7] These findings could indicate that "dual cleavage" is necessary to degrade and liberate peptides from membrane.

EFFECTS OF PS FAD MUTATION ON INTRAMEMBRANOUS ENDOPROTEOLYSIS OF NOTCH-1 AGREE WITH THOSE OF βAPP

An important finding is that, similar to the pathological cut of βAPP, the precision of the γ-cleavage-generating C-terminus of Nβ is affected by FAD-associated PS1/2 mutations (Fig. 4 and data not shown).[6] Fig. 4 summarizes how dual γ-cleavage of Notch-1/βAPP and transmembrane domain are modified by PS1 L166P pathological mutation. Cleavage efficiency of neither S4 of Notch-1 nor γ40 of βAPP is changed by the mutation[31] (Okochi unpublished observation), whereas the precision of both cuts is affected,[1,6] which leads to increased generation of C-terminally elongated Nβ/Aβ, derived from minor cleavages occurring more C-terminally than the major cuts. In K293 cells expressing the PS1 L166P mutant, γ42/43 (Aβ numbering) cleavage increases but not that of γ40 of βAPP (Moehlmann PNAS). Similarly, Notch S4 cleavage at S4-1733–5 occurring more C-terminally than major S4-1731 increases in the cell.[6] In any case the PS mutant causes C-terminus Aβ-like peptide (Aβ/Nβ) elongation.

Both S3 of Notch-1 and γ49 of βAPP are the other cleavage sites of dual intramembranous proteolysis at the cytoplasmic border of membrane. Importantly, efficiency of both Notch and BAPP endoproteolysis is decreased by the mutation.[31] That is, both NICD and AICD generation decrease in the mutant expressing cells. Considering that the mutant does not cause decreased generation of Nβ/Aβ reflecting S4/γ40 cleavage, mutant effects on S4/

γ40 and S3/γ49 cleavages are distinct. In addition to major γ49 cleavage, a minor cut occurs at the γ48 site of the single amino acid N-terminus in the case of βAPP. However, since the γ48 cut level was not affected by the mutation in our study, relative cleavage efficiency at γ48 to γ49 looks to be up-regulated. Collectively, PS1 L166P mutant effects on γ-cleavage of βAPP and Notch-1 are extremely similar. Considering that both βAPP and Notch-1 undergo intramembranous endoproteolysis by an indistinguishable dual cleavage mechanism, we propose that PS1 pathogenic mutation affects the cleavages of βAPP and Notch-1 through an unknown identical mechanism.

Aβ-LIKE PEPTIDES AS A SURROGATE OF Aβ

Almost 20 years ago biochemical analysis of the AD brain revealed Aβ as a major constituent of senile plaque. However, before us, other Aβ-like peptide sequences have not been identified. These facts suggest that the characteristic of Aβ to accumulate in senile plaque might be specific to Aβ among Aβ-like peptides. In this case, the level of Aβ-like peptides, such as Nβ, could be used as a surrogate of Aβ. For example, by measuring the relative level of Nβ1733–35 to that of major Nβ1731 in CSF or peripheral blood, it may be possible to determine the Aβ42/40 generation ratio (see also Fig. 5). Or Aβ deposition leading to AD may gradually take place over a number of years. It is likely that, through the process, γ-secretase activity is up-regulated[32] or the precision of γ-cleavage in the brain is affected.[1] Therefore, by measuring the level of Aβ-like peptide as a surrogate of Aβ in healthy individuals, it may be possible to assess how fast and how much Aβ is going to accumulate in brain (Fig. 5).

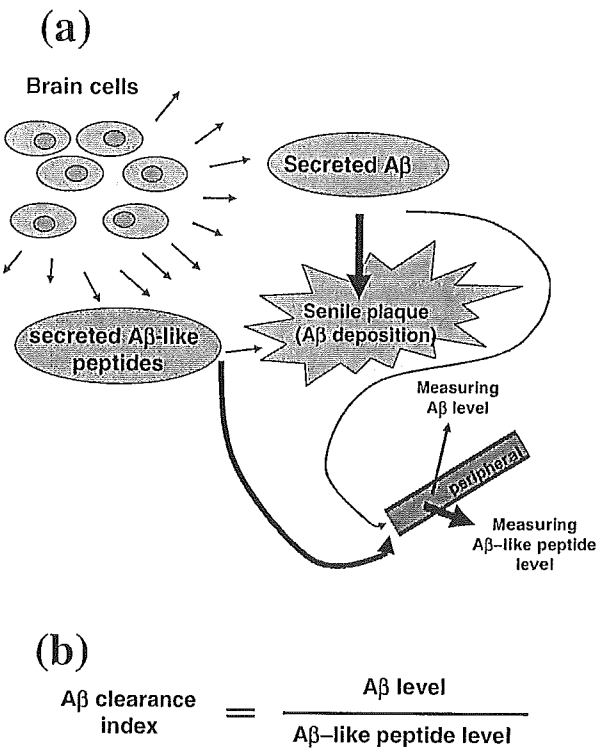

Figure 5 (a) Assessment of activity and precision of γ-secretase by measuring Aβ like peptide as surrogate of Aβ. The figure indicates our proposal. In brain of AD or those in whom the AD pathological process has already started, extracellularly secreted Aβ is trapped within brain when accumulated in senile plaques and other regions. Because of this, a lower level of Aβ in peripheral blood than that generated is recovered. On the other hand, Aβ-like peptide produced by the same PS/γ-secretase mechanism as Aβ does not accumulate in plaques, which indicates that most of it is basically released in peripheral blood and the peripheral blood level reflects its generation. (b) Assessment of Aβ accumulation speed by Aβ clearance index. In the case that generation of Aβ-like peptide reflects PS/γ-secretase activity exactly, relative reduction of Aβ to Aβ-like peptides in peripheral blood indicates Aβ accumulation in brain.

ACKNOWLEDGMENTS

We wish to thank our colleagues at the laboratory of the Department of Neuropsychiatry, Laboratory for Biochemistry, Osaka University Graduate School of Medicine, especially Dr Nuripa Aidaralieba, Kana Horinouchi, and Yumi Satoh for their technical assistance. This work was supported by grants from the Ministry of Education, Science, Culture and Sports (14017060 and 14770499 to M.O) and the Ministry of Health and Welfare (14121601 to M.T and M.O and 13080101 to M.T).

REFERENCES

1 Selkoe DJ. Alzheimer's disease. genes, proteins, and therapy. *Physiol Rev* 2001; *Physiol Rev*: 741–766. [Review.]
2 Haass C, Schlossmacher MG, Hung AY *et al.* Amyloid beta-peptide is produced by cultured cells during normal metabolism. *Nature* 1992; **359**: 322–325.
3 Shoji M, Golde TE, Ghiso J *et al.* Production of the Alzheimer amyloid beta protein by normal proteolytic processing. *Science* 1992; **258**: 126–129.
4 Steiner H & Haass C. Intramembrane proteolysis by presenilins. *Nat Rev Mol Cell Biol* 2000; **1**: 217–224. [Review.]
5 Teunissen CE, de Vente J, Steinbusch HW, De Bruijn C. Biochemical markers related to Alzheimer's dementia in serum and cerebrospinal fluid. *Neurobiol Aging* 2002; **23**: 485–508.

6 Okochi M, Steiner H, Fukumori A *et al.* Presenilins mediate a dual intramembranous gamma-secretase cleavage of Notch-1. *EMBO J* 2002; **21**: 5408–5416.

7 Lammich S, Okochi M, Takeda M *et al.* Presenilin dependent intramembrane proteolysis of CD44 leads to the liberation of its intracellular domain and the secretion of an Abeta-like peptide. *J Biol Chem* 2002; **277**: 44754–44759.

8 Mumm JS & Kopan R. Notch signaling: from the outside in. *Dev Biol* 2000; **228**: 151–165.

9 Brown MSYeJ, Rawson RB, Goldstein JL. Regulated intramembrane proteolysis: A control mechanism conserved from bacteria to humans. *Cell* 2000; **100**: 391–398.

10 Ye J, Rawson RB, Komuro R, Chen X, Dave UP, Prywes R, Brown MS, Goldstein JL. ER stress induces cleavage of membrane-bound ATF6 by the same proteases that process SREBPs. *Mol Cell* 2000; **6**: 1355–1364.

11 Yoshida H, Matsui T, Yamamoto A, Okada T, Mori K. XBP1 mRNA is induced by ATF6 and spliced by IRE1 in response to ER stress to produce a highly active transcription factor. *Cell* 2001; **107**: 881–891.

12 Mizutani T, Taniguchi Y, Aoki T, Hashimoto N, Honjo T. Conservation of the biochemical mechanisms of signal transduction among mammalian Notch family members. *Proc Natl Acad Sci USA* 2001; **98**: 9026–9031.

13 Saxena MT, Schroeter EH, Mumm JS, Kopan R. Murine notch homologs (N1–4) undergo presenilin-dependent proteolysis. *J Biol Chem* 2001; **276**: 40268–40273.

14 Naruse S, Thinakaran G, Luo JJ *et al.* Effects of PS1 deficiency on membrane protein trafficking in neurons. *Neuron* 1998; **21**: 1213–1221.

15 Lee HJ, Jung KM, Huang YZ, Bennett LB, Lee JS, Mei L, Kim TW. Presenilin-dependent gamma-secretase-like intramembrane cleavage of ErbB4. *J Biol Chem* 2002; **277**: 6318–6323.

16 Marambaud P, Shioi J, Serban G *et al.* A presenilin-1/ gamma-secretase cleavage releases the E-cadherin intracellular domain and regulates disassembly of adherens junctions. *EMBO J* 2002; **21**: 1948–1956.

17 May P, Reddy YK, Herz J. Proteolytic processing of low density lipoprotein receptor-related protein mediates regulated release of its intracellular domain. *J Biol Chem* 2002; **277**: 18736–18743.

18 Okamoto I, Kawano Y, Murakami D *et al.* Proteolytic release of CD44 intracellular domain and its role in the CD44 signaling pathway. *J Cell Biol* 2001; **155**: 755–762.

19 Kim DY, Ingano LA, Kovacs DM. Nectin-1alpha, an immunoglobulin-like receptor involved in the formation of synapses: Is a substrate for presenilin/gamma-secretase-like cleavage. *J Biol Chem* 2002; **277**: 49976–49981.

20 Ikeuchi T & Sisodia SS. The Notch ligands, Delta1 and Jagged2, are substrates for presenilin-dependent 'gamma-secretase' cleavage. *J Biol Chem* 2003; **278**: 7751–7754.

21 LaVoie MJ & Selkoe DJ. The Notch ligands, Jagged and Delta, are sequentially processed by alpha-secretase and presenilin/ gamma-secretase and release signaling fragments. *J Biol Chem* 2003; **278**: 34427–34437.

22 Taniguchi Y, Kim SH, Sisodia SS. Presenilin-dependent 'gamma-secretase' processing of deleted in colorectal cancer (DCC). *J Biol Chem* 2003; **278**: 30425–30428.

23 Jung KM, Tan S, Landman N *et al.* Regulated intramembrane proteolysis of the p75 neurotrophin receptor modulates its association with the TrkA receptor. *J Biol Chem* 2003; **278**: 42161–9.

24 Araki Y, Tomita S, Yamaguchi H *et al.* Novel cadherin-related membrane proteins, Alcadeins, enhance the X11-like protein-mediated stabilization of amyloid beta -protein precursor metabolism. *J Biol Chem* 2003; **278**: 49448–58.

25 Schulz JG, Annaert W, Vandekerckhove J, Zimmermann P, De Strooper B, David G. Syndecan 3 intramembrane proteolysis is presenilin/gamma -secretase-dependent and modulates cytosolic signaling. *J Biol Chem* 2003; **278**: 48651–7.

26 Li X & Greenwald I. Membrane topology of the C. elegans SEL-12 presenilin. *Neuron* 1996; **17**: 1015–1021.

27 Takasugi N, Tomita T, Hayashi I *et al.* The role of presenilin cofactors in the gamma-secretase complex. *Nature* 2003; **422**: 438–41.

28 Edbauer D, Winkler E, Haass C, Steiner H. Presenilin and nicastrin regulate each other and determine amyloid beta-peptide production via complex formation. *Proc Natl Acad Sci USA* 2002; **99**: 8666–8671.

29 Haass C & Steiner H. Alzheimer disease gamma-secretase. A complex story of GxGD-type presenilin proteases. *Trends Cell Biol* 2002; **12**: 556–562.

30 Wong PC, Zheng H, Chen H, Becher MW *et al.* Presenilin 1 is required for Notch1 and DII1 expression in the paraxial mesoderm. *Nature* 1997; **387**: 288–292.

31 Moehlmann T, Winkler E, Xia, X *et al.* Presenilin-1 mutations of leucine 166 equally affect the generation of the Notch and APP intracellular domains independent of their effect on Abeta 42 production. *Proc Natl Acad Sci USA* 2002: **99**: 8025–30.

32 Ikeuchi T, Dolios G, Kim SH, Wang R, Sisodia SS. Familial Alzheimer disease-linked presenilin 1 variants enhance production of both Abeta 1–40 and Abeta 1–42 peptides that are only partially sensitive to a potent aspartyl protease transition-state inhibitor of 'gamma-secretase'. *J Biol Chem* 2003; **278**: 7010–8.